

Denoising ohmic Contact Image Using Spatial Filter

B. N. Shashikala
Research Scholar
MGR University
Chennai, India
shashikala.bn@rediffmail.com

B. S. Nagabhushana
BMS College of Engineering
Bangalore

Abstract

The surface study of Ti/Al and Ti/Al/Ni/Au films deposited by electron beam evaporation on n type GaN were characterized by employing Scanning Electron Microscope. The surface morphology of Ti/Al and Ti/Al/Ni/Au contacts were studied as a function of the annealing process conditions using image processing techniques. Scanning Electron Microscope images need to be preprocessed before finding porosity where different types of noises are filtered. This paper focuses on how different image filtering techniques contributes in denoising GaN image so that pores can be easily identified and accurate values of porosity can be found.

Keywords: GaN, ohmic contact, Power signal, surface morphology

1. Introduction

Group III-V semiconductors, especially Gallium Nitride (GaN), are highly attractive materials for high speed electrical and optoelectronics devices such as laser diodes, light-emitting diodes and high electron mobility transistors [1,2]. GaN devices are of interest in the development of high temperature/high power electronics at microwave frequencies. To fabricate high performance devices, low resistance ohmic contacts with good surface morphologies are essential. Several metallization schemes such as Ti, Ti/Al, Ti/Al/Cu/Au, Ti/Al/Pt/Au, Ti/Al/Ti/Au, Ti/Al/Ni/Au, Ti/Al/Pd/Au, Ti/Al/Mo/Au, Ti/Al/Re/Au, etc., have been reported to form ohmic contacts to n-GaN [3-11]. Investigations on these contacts have indicated that the formation of TiN at the interface may be important for ohmic contact formation due to its low work function and the formation of nitrogen vacancies in the GaN below the contact layer by a reaction of Ti with GaN. The use of Ti/Al instead of Ti decreases the contact resistivity further by forming AlN at the interface in addition to TiN.

In this work, the surface morphology of Ti/Al and Ti/Al/Ni/Au ohmic contacts to n-GaN were examined with the use of Scanning Electron Microscope (SEM). SEM images are used to study the thin film of Ti/Al and Ti/Al/Ni/Au contacts to n-GaN layer using image processing techniques. In this paper various filters Disk, Gaussian, Motion, Average, unsharp, Median, Max, Min and Adaptive Wiener filters are used to remove noise from ohmic contact images and also compare results with estimation of parametric principles like Mean Square Error (MSE) and Peak Signal Noise Ratio (PSNR). The experiment results shows that Adaptive Wiener and Gaussian filter are the best filter for ohmic contact images. This paper discusses the surface property of Ti/Al and Ti/Al/Ni/Au thin film by spatial filtering techniques.

2. Image Processing Techniques on Ohmic Contact Surface

Fig. 1 shows the block diagram for finding porosity on ohmic contact surface SEM images. Image acquisition is done using SEM. Second step is preprocessing, which involves denoising, debris removal, removal of salt and pepper noises. Since porosity is based on minute pores of nano sizes on surface, one has to carefully select filters.

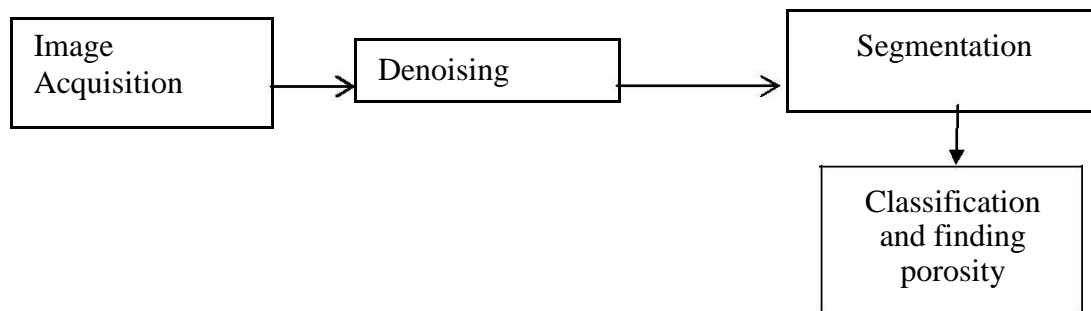


Figure 1: Block diagram for finding porosity on Ohmic contact surface SEM images

Filter is a technique that discriminates according to one or more attributes at its input, what passes through it. For example, color filters absorb light at certain wave lengths. It passes signals with frequency components in some bands and attenuate signals in other frequency bands. These techniques use operations like convolution and correlation.

Correlation is an operation which involves filtering a mask over an image. The Correlation operator \diamond of filter $w(p,q)$ of image of size $(m \times n)$ with an image $I(p,q)$ is given by [12]

$$w(p,q) \diamond I(p,q) = \sum_{s=-a}^a \sum_{t=-b}^b w(s,t)I(p+s,q+t) \quad (1)$$

where a_m is a mask over an image, $w(p,q)$ is a filter of size (m,n) , $I(p,q)$ an image.

Convolution is almost same as correlation but the mask reflected about both axes. Mask is rotated by 180° . Convolution operator $*$ of filter $w(p,q)$ of size $m \times n$ with image $I(p,q)$ is given by

$$w(p,q) * I(p,q) = \sum_{s=-a}^a \sum_{t=-b}^b w(s,t)I(p-s, q-t) \quad (2)$$

Convolution is used in time domain filtering where as multiplication is used in frequency domain filtering. Spatial filters consider image as a grid of pixels. It directly manipulates pixels in an image. The values of neighborhood pixels are important there. This uses convolution. This changes pixels in the region of interest by its neighbor pixel values. There are three types of spatial filters used.

1. Linear
2. Non linear
3. Adaptive.

2.1 Performance Measures

Mean Square Error (MSE)

The MSE denotes the collective squared error between the compressed and the original image, whereas PSNR denotes an amount of the highest error. The low value of MSE means the error is low. To compute the PSNR, the block first computes the mean-squared error using the subsequent equation:

$$MSE = \frac{1}{mn} \sum_{i=0}^{m-1} \sum_{j=0}^{n-1} [I(i,j) - K(i,j)]^2 \quad (3)$$

where m and n are the number of rows and columns in the input images, respectively.

Peak Signal-to-Noise Ratio (PSNR)

PSNR is the evaluation standard of the reconstructed image quality, and is an important feature. The small value of PSNR means that image is poor quality. PSNR is defined as follow [13,14]:

$$PSNR = 10 \cdot \log_{10} \left(\frac{MAX_I^2}{MSE} \right) \quad (4)$$

where 255 is maximum possible value that can be attained by the image signal. Ideally it is infinite. Practically it is in the range of 25 to 40 db.

3 Experiment

The experimental procedure of this work consists of three important steps: the fabrication of ohmic contact structures, the characterization of the structures using the

SEM, and analysis of the images through the extraction of the more accurate morphology of the structures.

3.1 Fabrication Procedure

A doped n-type (N_D^+ approximately $3 \times 10^{18} \text{ cm}^{-3}$ by Hall measurement) GaN layer of $5 \mu\text{m}$ grown by MOCVD on c-plane sapphire substrate was used for the experiment. Prior to metal deposition, a sample was cleaned in trichloroethylene (TCE) to degrease and then treated using acetone for further cleaning. The sample was then immersed in isopropyl alcohol (IPA) for complete removal of organic solvents. The sample was then well rinsed in deionized water (DI) and ready for removal of ionic contaminants and native oxide. The sample was then immersed in an equally proportioned solution of dilute HCl in deionized water. After this treatment for 5 minutes, the sample was rinsed again in DI water and blow dried using N_2 gas. The electron beam (e-beam) evaporator was evacuated to a base pressure of about 5×10^{-6} mbar prior to deposition. The composite metal layers were Ti/Al (20nm/100nm) and Ti/Al/Ni/Au (20nm/100nm/20nm/100nm). All the metals were deposited by electron beam evaporation at 50°C . The metal contacts were fabricated with standard photolithographic technique with a positive photo resist. The metal lift off was followed by a Rapid Thermal Anneal (RTA) in a N_2 ambient. The Ti/Al ohmic contact samples were annealed at 600°C , 700°C , 800°C and 900°C in an RTA furnace for 1 min in a N_2 ambient. The Ti/Al/Ni/Au ohmic metallization samples were annealed at 750°C , 800°C , 850°C , and 900°C in an RTA furnace for 1 min in a N_2 ambient. The influence of the annealing process on the surface morphology of Ti/Al and Ti/Al/Ni/Au ohmic contacts to GaN were examined with the use of a SEM.

3.2 Analysis of SEM Images Using Image Processing Techniques

SEM image is saved as JPEG format. Later image is input into MATLAB environment using imread function. Images are converted into gray scale for thresholding. Various filtering techniques were used to select preprocessing method suitable for these images. PSNR and MSE are the different metrics used to measure the performance of different filtering techniques. The different filtering techniques were applied on 8 images of Ti/Al and Ti/Al/Ni/Au materials, where four images of each material were taken at different temperature. For each filtering technique, both metrics values and image output are recorded. Based on metric, the best suitable filtering technique was decided.

4 Results and Discussion

Fig. 2 shows the top view SEM images of surface morphology of the Ti/Al ohmic contact after annealing at various temperatures 600°C , 700°C , 800°C and 900°C for 60s. Fig. 3 shows the top view SEM images of surface morphology of the Ti/Al/Ni/Au ohmic contact after thermal annealing at various temperatures for 60s.

An increase in annealing temperature resulted in the decrease in the density of agglomerates and leads to metal inter diffusion and alloying. This work aims to present the structural characterization of the ohmic contact to the n-GaN based on the

filtering techniques applied to SEM images. The sample images studied in this paper are of the same magnification (5000). Various image filtering techniques such as Disk, Gaussian, Motion, Average, Unsharp, Median, Max, Min and Adaptive Wiener in spatial filtering were implemented using MATLAB platform. PSNR and MSE are the different metrics used to measure the performance of different filtering techniques. The filtering techniques were applied on 8 images of Ti/Al and Ti/Al/Ni/Au materials. The performance of all these image filtering techniques are analyzed for a set of Ti/Al and Ti/Al/Ni/Au ohmic contact images and results are presented in tables 1 and 2, respectively.

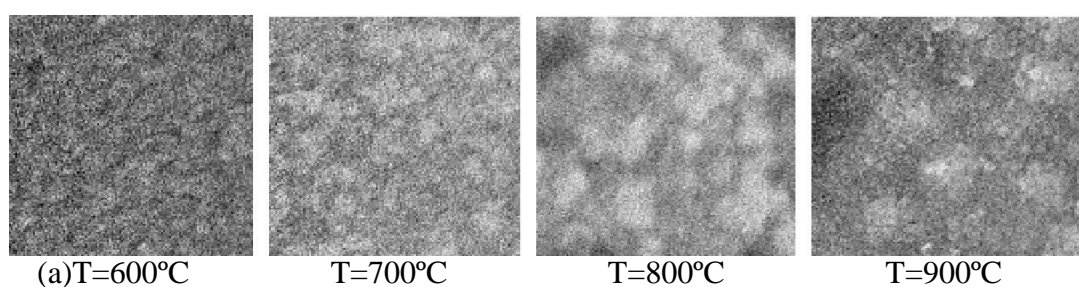


Figure 2: SEM images of the ohmic contact Ti/Al after thermal annealing at various temperatures for 60s.

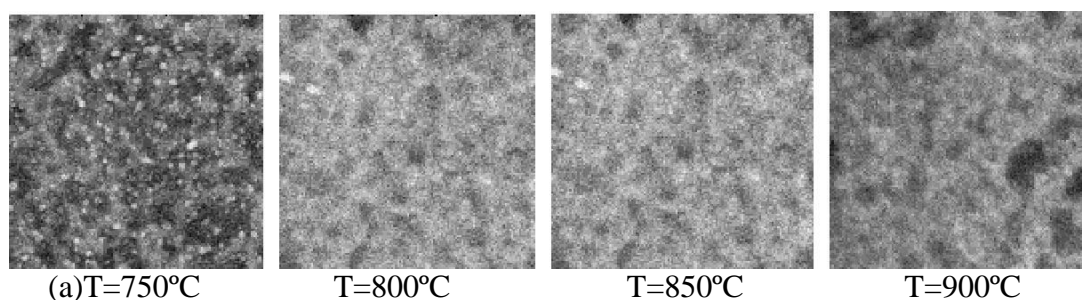


Figure 3: SEM images of the ohmic contact Ti/Al/Ni/Au after thermal annealing at various temperatures for 60s.

4.1 Metrics Values for Spatial Filters

Table 1 shows the variation of PSNR of Ti/Al ohmic contact versus annealing temperature for Disk, Gaussian, Motion, Average, Unsharp, Median, Max, Min and Adaptive Wiener in spatial filtering techniques. Peaks at 600°C and 800°C of Ti/Al ohmic contact represent more noise is filtered in the image and has high PSNR. Valleys at 700°C and 900°C represent less noise is filtered in the image and have low PSNR. The size of the kernel filter and coefficients are fixed and cannot be adapted to a given image in Gaussian, Motion, Average and Median filters. An adaptive Wiener provides a robust solution that is adaptable to the varying noise levels of these images. Adaptive Wiener gives better PSNR than other filtering techniques for Ti/Al ohmic contact.

Table 1: PSNR for Ti/Al ohmic contact

Temperature (°C)	Disk	Gaussian	Motion	Average	Unsharp	Median	Max	Min	Adaptive Wiener
600	26.50	27.65	27.04	26.61	16.55	27.15	19.35	20.75	27.25
700	20.28	21.30	20.94	20.41	15.20	20.57	13.22	14.96	21.70
800	24.44	26.22	25.37	24.85	19.29	26.07	17.64	18.85	26.02
900	23.96	24.69	24.33	24.09	17.39	24.03	16.89	18.03	24.97

Table 2: PSNR for Ti/Al/Ni/Au ohmic contact

Temperature (°C)	Disk	Gaussian	Motion	Average	Unsharp	Median	Max	Min	Adaptive Wiener
750	23.70	25.07	24.56	23.97	15.33	24.33	16.72	18.03	24.87
800	25.50	26.94	26.75	26.05	18.11	27.38	18.47	19.89	27.99
850	25.27	26.56	26.16	25.54	16.72	25.42	18.39	19.21	26.35
900	25.30	27.75	26.19	25.88	16.82	25.86	18.41	19.81	26.84

Table 3: MSE for Ti/Al ohmic Contact

Temperature (°C)	Disk	Gaussian	Motion	Average	Unsharp	Median	Max	Min	Adaptive Wiener
600	255	255	255	255	219.70	254.99	255	253.48	255
700	255	255	255	255	252.19	254.99	255	253.75	255
800	255	255	255	255	253.29	254.99	255	253.75	255
900	255	255	255	255	253.34	254.99	255	253.75	255

Table 4: MSE for Ti/Al/Ni/Au ohmic contact

Temperature (°C)	Disk	Gaussian	Motion	Average	Unsharp	Median	Max	Min	Adaptive Wiener
750	255	255	255	255	254.80	254.99	255	253.75	255
800	255	255	255	255	249.53	254.99	255	253.75	255
850	255	255	255	255	254.58	254.99	255	253.75	255
900	255	255	255	255	253.48	254.99	255	253.75	255

The specific contact resistance was determined from plots of the measured resistance versus the spacing between the circular transmission line method pads. Measurements showed that the specific contact resistances of Ti/Al after anneal varied in the range of 2×10^{-4} to $8 \times 10^{-4} \Omega \text{ cm}^2$. The variation in the contact resistance with increasing annealing temperature is believed to be from an increase in thermal inter diffusion at the interface between the deposited metals and GaN. The highest PSNR and lowest specific contact resistance was obtained at 600 °C.

Fig. 3 shows the top view SEM images of surface morphology of the Ti/Al/Ni/Au ohmic contact after thermal annealing at various temperatures for 60s. The grains agglomeration appeared at 750°C. As the annealing temperature was increased from 750°C to 900°C in steps of 50°C, the agglomerates migrated on the surface and

coalescence into larger agglomerates. Thus, the thermal annealing process significantly changes the morphology of the ohmic contact and influences the chemical composition of the surface of both Ti/Al and Ti/Al/Ni/Au contacts. Table 2 shows the variation of PSNR of Ti/Al/Ni/Au ohmic contacts versus annealing temperature for Disk, Gaussian, Motion, Average, Unsharp, Median, Max, Min and Adaptive Wiener in spatial filtering techniques. Peaks at 800°C and 900°C of Ti/Al/Ni/Au ohmic contact represent more noise is filtered in the image and has high PSNR. Valleys at 750°C and 850°C represent less noise is filtered in the image and have low PSNR. Adaptive Wiener gives better PSNR than other edge detection for Ti/Al/Ni/Au ohmic contact.

Measurements showed that the specific contact resistance of Ti/Al/Ni/Au ohmic contact after anneal varied in the range of 2×10^{-5} to $8 \times 10^{-5} \Omega \text{ cm}^2$. The highest PSNR and lowest specific contact resistance was obtained at 800 °C for Ti/Al/Ni/Au ohmic contact. It is noteworthy that the Ti/Al/Ni/Au contact show better electrical properties than the Ti/Al contacts. Adaptive Wiener gives better PSNR for Ti/Al/Ni/Au ohmic contact than Ti/Al ohmic contact.

As shown in Fig. 2 and Fig. 3, the surface of the ohmic contacts gets quite rough due to many grooves produced on the surface after annealing at high temperature. A rough surface of ohmic contact is bad for reliability and stability. The roughness is due to the Al existing in the ohmic contact schemes, which does not react completely and is subject to melting at these high annealing temperatures.

5 Conclusions

Ti/Al and Ti/Al/Ni/Au ohmic contacts were deposited on n-type GaN and annealed at various temperatures for 60s have been compared in terms of specific contact resistance and surface morphology. The variation of PSNR of Ti/Al and Ti/Al/Ni/Au ohmic contacts versus annealing temperature for Disk, Gaussian, Motion, Average, Un sharp, Median, Max, Min and Adaptive Wiener in spatial filtering techniques were studied. Gaussian and Adaptive Wiener gives better PSNR for Ti/Al and Ti/Al/Ni/Au ohmic contacts. Adaptive Wiener gives better PSNR for Ti/Al/Ni/Au ohmic contact than Ti/Al ohmic contact. Thus Ti/Al/Ni/Au ohmic contacts may be preferred for high temperature and high power devices on GaN.

Acknowledgment

The authors would like to thank the professors and staff members of the Center of Excellence in Nano electronics (CEN) for their support during the fabrication process.

The experiments in this paper were carried out at Indian Institute of Technology Bombay and Indian Institute of Science Bangalore under the Indian Nanoelectronics Users Program.

References

- [1] X. Zhang, A. Saxler, P. Kung, M. Razeghi, D. Walker, and J. Xu, *Applied Physics Letters* 68(15), 2100(1996).
- [2] R. Stall, S. Liang, Y. Lu, C. Joseph, I. Ferguson, C.A. Tran, R.F. Karliceck, and Z.C. Feng, *Materials Science and Engineering B* 50(1), 311(1997).
- [3] N. A. Papanicolaou, M. V. Rao, J. Mittereder, and W. T. Anderson, *Journal of Vacuum Science & Technology B* 19, 261(2001).
- [4] M. E. Lin, Z. Ma, F. Y. Huang, Z. F. Fan, L. H. Allen, and H. Morkoc, *Appl. Phys. Lett.* 64 (8), 1003(1994).
- [5] Cong Wang and Nam-Young Kim, *Nanoscale Research Letters*, (2012).
- [6] V. Rajagopal Reddy and C. K. Ramesh, *Journal of Optoelectronics and Advanced Materials*, 6(1), 177(2004).
- [7] H. C. Lee, J. W. Bae, and G. Y. Yeom, *Journal of the Korean Physical Society*, 51(3),1046(2007).
- [8] Deepak Selvanathan, Fiti M. Mohammed, Asrat Tesfayesus and Ilesanmi Adesida, *Journal of Vacuum Science & Technology B* 22(5), 2409(2004).
- [9] L. Dobos, B. Pecz, L. Toth, Zs. J. Horvath, Z. E. Horvath, A. Toth, E. Horvath, B. Beaumont, and Z. Bougrioua, *Applied Surface Science*, 253, 655(2006).
- [10] D. Selvanathan, L. Zhou, V. Kumar, and I. Adesida, *Pyhs. Stat. Sol.*, 2, 583(2002).
- [11] Su Jin Kim, Tae Yang Nam, and Tae Geun Kim, *IEEE Electron Device Letters*, 32(2), 149(2011).
- [12] R.C. Gonzalez and R.C. Woods, *Digital Image Processing*, 3rd edn., (2008).
- [13] Z. Wang, A. C. Bovik, H. R. Sheikh, and E. P. Simoncelli, "Image quality assessment: From error visibility to structural similarity," *IEEE Trans. Image Process.*, 13(4), 600(2004).
- [14] H. R. Sheikh and A. C. Bovik, "Image information and visual quality," *IEEE Trans. Image Process.*, 15(2), 430(2006).
- [15] Zhou Wang, Alan C. Bovik , "A Universal Image Quality Index", *IEEE Signal Processing Letters*, 9(3), 81(2002).